

# MULTI-SCALE TIME-CHANGED BIRTH PROCESSES FOR PRICING MULTI-NAME CREDIT DERIVATIVES

ERHAN BAYRAKTAR AND BO YANG

ABSTRACT. We develop two parsimonious models for pricing multi-name credit derivatives. We derive closed form expression for the loss distribution, which then can be used in determining the prices of tranche and index swaps and more exotic derivatives on these contracts. Our starting point is the model of [3], which takes the loss process as a time changed birth process. We introduce stochastic parameter variations into the intensity of the loss process and use the multi-time scale approach of [6] and obtain explicit perturbation approximations to the loss distribution. We demonstrate the competence of our approach by calibrating it to the CDX index data.

## 1. INTRODUCTION

Copulas have been the standard approach in the financial industry for creating correlation structures and pricing multi-name credit derivatives. However, copula models have some well known drawbacks. Most importantly, no single copula model can fit the market data of several tranches at the same time. It is usually the case that some practitioners have to interpolate between models to price non-standard tranches, which may introduce arbitrage opportunities. Moreover copula models are static. They do not take into account the time evolution of joint default risks, therefore cannot be used to price more exotic, multi-period instruments, such as tranche forwards and tranche options. This has motivated recent work in developing alternative approaches to multi-name credit risk modeling. Several recent papers proposed a top-down approach, in which one models the portfolio loss process directly as a jump process, whose default intensity  $\lambda_t$  represents the conditional rate of occurrence of the next default. We are interested in the top-down framework proposed in [3], in which the portfolio loss process is modeled as a time-changed birth process. Under this general setting, [3] analyzed and implemented a particular parametric specification, where the time change activity rate is a CIR process. The advantage of this model over other top-down models is its tractability: the loss distribution and hence the tranche prices can be expressed in closed form. On the other hand, there are limitations of this model, as also pointed out in [3]. Between default events, the default intensity volatility and mean reversion level are constant. These parameters have to be dependent on the number of defaults  $N$ , and the dependence is simple: they increase as  $N$  increases. This undesired feature is a result of using the birth process, whose intensity is

---

*Key words and phrases.* Pricing multiname credit derivatives, pertubation approximation, multiple time scales, time changed birth processes, index/tranche swap, calibration.

This research is supported in part by the National Science Foundation.

This version: Feb 12, 2009. To appear in Applied Mathematical Finance, 2009.

E. Bayraktar is with the Department of Mathematics, University of Michigan, Ann Arbor, MI 48109; erhan@umich.edu.

B. Yang is with Morgan Stanley, 1585 Broadway, 3rd Floor, New York, NY 10036.

always increasing, as a process to be time changed. The model turns out to be a special specification of the class of affine point process models introduced in [4], but with gained tractability at the cost of reduced flexibility.

In this paper, we propose to address those issues by introducing stochastic parameter fluctuations to the dynamics of the intensity process  $\lambda_t$ . We then use the approach of [6] to develop asymptotic approximations for the loss distribution. Two different models are proposed in Sections 3 and 4, respectively. The motivation is to go beyond the affine family of models and bring in more flexibility. By properly specifying the fast and slow factors, we are able to keep the tractability and improve the fit to the market data. Multi-scale stochastic modeling for multi-name credit derivatives is also discussed in [7], which considers stochastic parameter extension to a bottom up model where individual default intensities are given by correlated Ornstein-Uhlenbeck processes. We compare our models' performance to the performance of the particular model introduced in Section 3 of [7].

We calibrate our models to the CDX index data and demonstrate that the introduction of the stochastic parameters into the framework of [3] improves the fit to the market data (see Section 5 and Tables 1 and 3). This improvement does not at a high computational cost since the corrections to the loss distribution can be explicitly calculated in the two models we propose here. The rest of the paper is organized as follows: We describe the top-down approach introduced in [3] in Section 2 and describe the relationship between the prices of tranche and index swaps and the loss distribution. In Section 3, we study a stochastic volatility extension. In Section 4, we discuss an extension, in which the stochastic mean reversion level is stochastic. In Section 5, we implement the calibration of the models to the market data and analyze the stability of the calibrated parameters (see Figures 1, 3, 4, 5; and Tables 1-3). In Figure 2 we plot the model predicted prices of more exotic contracts written on the tranches.

## 2. MODELING

**2.1. Time-Changed Birth Process.** We consider the model proposed in [3], in which correlated default arrivals are modeled directly under a risk-neutral pricing measure through a time-changed birth process  $N$ . More precisely, suppose that  $N^0$  is a birth process defined on the probability space  $(\Omega, \mathcal{G}, P)$  with a right-continuous and complete filtration  $\mathbb{F} = (\mathcal{F}_t)_{t \geq 0}$ . Its intensity is given by

$$\lambda_t^0 = \theta_1 + \theta_2 N_t^0.$$

The time-changed birth process is defined by

$$(2.1) \quad N_t = N_{T_t}^0 \quad \text{where} \quad T_t = \int_0^t X_s ds.$$

Let  $\mathbb{G} = (\mathcal{G}_t)_{t \geq 0}$  be the right-continuous and complete filtration generated by the stopping time sigma-fields  $\mathcal{F}_{T_t}$ . Therefore,  $(\mathcal{G}_t)_{t \geq 0}$  represents the information flow in the new time scale. We assume that the activity rate  $X$  is independent of the birth process  $N^0$ , and follows the dynamics:

$$dX_t = \kappa(\mu - X_t)dt + \sigma\sqrt{X_t}dW_t^0.$$

By (4) in [3], the intensity  $\lambda$  for process  $N$  is given by

$$\lambda_t = X_t(\theta_1 + \theta_2 N_t).$$

Due to the above specification of  $X$ ,  $N$  is a counting process whose intensity satisfies

$$(2.2) \quad d\lambda_t = \kappa(\mu\eta_t - \lambda_t)dt + \sigma\sqrt{\eta_t\lambda_t}dW_t^0 + \frac{\theta_2}{\eta_t}\lambda_t dN_t,$$

where  $\eta_t = \theta_1 + \theta_2 N_t$ . For a portfolio of credit securities that are issued by  $n$  names, we define  $N^n = N \wedge n$  to be the process that counts the number of defaults in the portfolio. Let

$$\lambda_t^n = \lambda_t 1_{\{N_t < n\}},$$

$\lambda^n$  be the intensity of  $N^n$ .

**2.2. Tranche and Index Swaps.** Tranche and Index swaps are based on an index portfolio with  $n$  constituent bonds with common maturity and common notional which we assume to be equal to  $1/n$ . We will assume the loss given default to be a constant and we will denote it by  $l$ . Under this assumption the cumulative loss process  $L^n$  is defined in terms of  $N^n$  by

$$L_t^n = \frac{lN_t^n}{n}.$$

A tranche swap is an insurance against losses between  $\underline{K} \in [0, 1]$  and  $\overline{K} \in [\underline{K}, 1]$ . For index swap,  $\underline{K} = 0$  and  $\overline{K} = 1$ . The protection buyer in the swap pays the seller an upfront fee in the amount of  $FK$  and a premium to the protection on future dates  $(t_1, \dots, t_i, \dots, t_M)$ , with  $t_M$  being the maturity of the contract. Let us denote the cumulative tranche loss at time  $t$  by

$$U_t = (L_t^n - \underline{K})^+ - (L_t^n - \overline{K})^+.$$

The amount of the premium paid at each payment date  $t_i$  is a fixed fraction  $spr$  (usually quoted as an annual rate) of  $K - U_{t_i}$ , the difference between the tranche notional and the cumulative tranche loss to  $t_i$ . The protection seller, on the other hand, compensates the protection buyer for the default losses that occur before the maturity of the contract. We assume that the compensation for a loss is paid at the very next premium payment date  $t_i$ . Therefore, the present value of the premium leg is

$$\text{premium}_{t,T} = spr \sum_{i=1}^M c_i e^{-r(t_i-t)} (K - \mathbb{E}[U_{t_i} | \mathcal{G}_t]) + F \cdot K,$$

where  $c_i$  is the day count fraction for period  $i$ . Usually, payments are made quarterly, and  $c_i = 0.25$ . The premium leg is defined differently for the index swap, in that it ignores the loss at default, i.e.,

$$\text{premium}_{t,T}^{index} = spr \sum_{i=1}^M c_i e^{-r(t_i-t)} \left( 1 - \frac{\mathbb{E}[N_{t_i}^n | \mathcal{G}_t]}{n} \right),$$

On the other hand, the present value of the protection leg is

$$\text{protection}_{t,T} = \sum_{i=1}^M e^{-r(t_i-t)} (\mathbb{E}[U_{t_i} | \mathcal{G}_t] - \mathbb{E}[U_{t_{i-1}} | \mathcal{G}_t]).$$

The tranche swap spread  $spr$  is determined, as for CDS spread, by equating the premium leg and the protection leg. We obtain

$$(2.3) \quad spr = \frac{\sum_{i=1}^M e^{-r(t_i-t)} (\mathbb{E}[U_{t_i}|\mathcal{G}_t] - \mathbb{E}[U_{t_{i-1}}|\mathcal{G}_t]) - F \cdot K}{\sum_{i=1}^M c_i e^{-r(t_i-t)} (K - \mathbb{E}[U_{t_i}|\mathcal{G}_t])}.$$

For the equity tranches (tranches with the lowest attachment points), the market convention is to charge an upfront payment from the protection buyer, while fixing the spread at certain level  $s^*$ , say 500bsp. In this case,

$$(2.4) \quad F = \frac{1}{K} \left[ \sum_{i=1}^M e^{-r(t_i-t)} (\mathbb{E}[U_{t_i}|\mathcal{G}_t] - \mathbb{E}[U_{t_{i-1}}|\mathcal{G}_t]) - s^* \sum_{i=1}^M c_m e^{-r(t_i-t)} (K - \mathbb{E}[U_{t_i}|\mathcal{G}_t]) \right].$$

is quoted. We will show that  $spr$  in (2.3) and  $F$  in (2.4) can be calculated explicitly. For this purpose, we compute  $\mathbb{E}_t[U_T]$ , which can be expressed using the distribution of  $N_T$  as follows

$$\mathbb{E}_t[U_T] = \sum_{k=0}^{n-N_t^n} U_T \left( \frac{l(k + N_t^n)}{n} \right) \mathbb{P}[N_T^n - N_t^n = k | \mathcal{G}_t],$$

in which

$$\mathbb{P}[N_T^n - N_t^n = k | \mathcal{G}_t] = \begin{cases} \mathbb{P}[N_T - N_t = k | \mathcal{G}_t] & \text{if } k < n - N_t^n \\ \mathbb{P}[N_T - N_t \geq k | \mathcal{G}_t] & \text{if } k = n - N_t^n \\ 0 & \text{if } k > n - N_t^n. \end{cases}$$

The probability distribution of  $N_T - N_t$  is given by

$$(2.5) \quad \mathbb{P}[N_T - N_t = k | \mathcal{G}_t] = \frac{\Gamma(C_t + k)}{\Gamma(C_t)k!} \sum_{m=0}^k (-1)^m \binom{k}{m} \mathcal{T}_{t,T}(\theta_1(m + C_t), 0),$$

where  $C_t = N_t + \frac{\theta_1}{\theta_2}$  and

$$(2.6) \quad \mathcal{T}_{t,T}(s, \xi) = \mathbb{E}_t \left[ e^{-s \int_t^T X_u du + i \xi X_T} | \mathcal{G}_t \right];$$

see [3].

**2.3. Tranche and Index Options.** Tranche and Index options are derivatives on the mark-to-market value which is defined as

$$M_{t,T}(spr, F) = \text{protection}_{t,T}(spr, F) - \text{premium}_{t,T}(spr, F).$$

These exotic derivatives allow investors to bet on the future spreads. The value of an option on a swap with payoff function  $h$ , maturity  $T$ , exercise date  $T^* < T$  and strike spread  $S$  and upfront rate  $F$  at time  $t$  is

$$\exp(-r(T^* - t)) \mathbb{E}[h(M_{T^*,T}(S, F)) | \mathcal{G}_t]$$

As it can be observed from the previous section,  $M_{T^*,T}(S, F)$  is function of  $N_{T^*}^n$  and  $X_{T^*}$ . We will show this dependence explicitly and write

$$\widetilde{M}_{T^*,T}(N_{T^*}^n, X_{T^*}; S, F) = M_{T^*,T}(S, F).$$

The expectation can be computed using joint of distribution of  $N_{T^*}^n - N_t^n$  and  $X_{T^*}$ :

$$\begin{aligned} \mathbb{E}[h(M_{T^*,T}(S, F))|\mathcal{G}_t] &= \mathbb{E}[h(\widetilde{M}_{T^*,T}(N_{T^*}^n, X_{T^*}; S, F))|\mathcal{G}_t] \\ &= \int_0^\infty \sum_{k=0}^{n-N_t^n} h(\widetilde{M}_{T^*,T}(k + N_t^n, x; S, F))\mathbb{P}[N_{T^*}^n - N_t^n = k, X_{T^*} \in dx|\mathcal{G}_t], \end{aligned}$$

in which

$$\mathbb{P}[N_{T^*}^n - N_t^n = k, X_{T^*} \in dx|\mathcal{G}_t] = \begin{cases} \mathbb{P}[N_{T^*} - N_t = k, X_{T^*} \in dx|\mathcal{G}_t] & \text{if } k < n - N_t^n \\ \mathbb{P}[N_{T^*} - N_t \geq k, X_{T^*} \in dx|\mathcal{G}_t] & \text{if } k = n - N_t^n \\ 0 & \text{if } k < n - N_t^n. \end{cases}$$

where the joint distribution of  $N_{T^*} - N_t$  and  $X_{T^*}$  is given by

$$(2.7) \quad \mathbb{P}[N_{T^*} - N_t = k, X_{T^*} \in dx|\mathcal{G}_t] = \frac{\Gamma(C_t + k)}{\Gamma(C_t)k!} \sum_{m=0}^k \frac{(-1)^m}{2\pi} \binom{k}{m} \int_{-\infty}^{\infty} \mathcal{T}_{t,T^*}(\theta_1(m + C_t), \xi) e^{-ix\xi} d\xi dx;$$

see [3].

### 3. STOCHASTIC VOLATILITY

In this section, we extend the top-down model described in the previous section to incorporate multi-scale stochastic volatility. Specifically, the activity rate  $X$  is modeled as the solution of

$$dX_t = \kappa(\mu - X_t)dt + f(Y_t, Z_t)\sqrt{X_t}dW_t^0,$$

in which  $f$  is a strictly positive, bounded, smooth function. The processes  $Y$  and  $Z$  are modeled by

$$\begin{aligned} dY_t &= \frac{1}{\epsilon} X_t(m - Y_t)dt + \frac{\nu\sqrt{2}}{\sqrt{\epsilon}} \sqrt{X_t}dW_t^1, \\ dZ_t &= \delta X_t c(Z_t)dt + \sqrt{\delta} \sqrt{X_t} g(Z_t)dW_t^2, \\ \mathbb{E}_t[dW_t^0 dW_t^i] &= \rho_i dt, \quad i \in \{1, 2\}, \quad \mathbb{E}_t[dW_t^1 dW_t^2] = \rho_{1,2} dt. \end{aligned}$$

in which  $\epsilon, \delta$  are small positive constants, and the functions  $c(z)$  and  $g(z)$  are assumed to be smooth. We assume that  $f^2(y, z) \leq 2\kappa\mu$  in order to guarantees the process  $X$  never hits zero; see [3]. With this specification, the intensity  $\lambda$  of the point process given by (2.1) has the dynamics

$$d\lambda_t = \kappa(\mu\eta_t - \lambda_t)dt + f(Y_t, Z_t)\sqrt{\eta_t\lambda_t}dW_t^0 + \frac{\theta_2}{\eta_t}\lambda_t dN_t,$$

where  $\eta_t = \theta_1 + \theta_2 N_t$ . Note that the intensity process inherits the stochastic volatility from the activity rate process  $X$ . We see from Section 2.2 that in order to obtain prices for multi-name credit derivatives,

we need to compute

$$\mathcal{T}_{t,T}(s, \xi) = \mathbb{E}_t \left[ e^{-s \int_t^T X_u du + i\xi X_T} \middle| \mathcal{G}_t \right] = u^{\epsilon, \delta}(t, x, y, z; s, \xi).$$

The function  $u^{\epsilon, \delta}$  satisfies the PDE

$$\begin{cases} \mathcal{L}^{\epsilon, \delta} u^{\epsilon, \delta} = 0 \text{ in } t < T, \\ u(T, x, y, z; s, \xi) = e^{i\xi x}, \end{cases}$$

where

$$\mathcal{L}^{\epsilon, \delta} := \frac{1}{\epsilon} \mathcal{L}_0 + \frac{1}{\sqrt{\epsilon}} \mathcal{L}_1 + \mathcal{L}_2 + \sqrt{\delta} \mathcal{M}_1 + \delta \mathcal{M}_2 + \sqrt{\frac{\delta}{\epsilon}} \mathcal{M}_3,$$

in which

$$\begin{aligned} \mathcal{L}_0 &:= x \left( \nu^2 \frac{\partial^2}{\partial y^2} + (m - y) \frac{\partial}{\partial y} \right) = x \tilde{\mathcal{L}}_0, \\ \mathcal{L}_1 &:= \sqrt{2\nu} \rho_1 f(y, z) x \frac{\partial^2}{\partial x \partial y}, \\ \mathcal{L}_2 &:= \frac{\partial}{\partial t} + \frac{1}{2} f^2(y, z) x \frac{\partial^2}{\partial x^2} + \kappa(\mu - x) \frac{\partial}{\partial x} - sx, \\ \mathcal{M}_1 &:= \rho_2 g(z) f(y, z) x \frac{\partial^2}{\partial x \partial z}, \\ \mathcal{M}_2 &:= x \left( c(z) \frac{\partial}{\partial z} + \frac{1}{2} g^2(z) \frac{\partial^2}{\partial z^2} \right), \\ \mathcal{M}_3 &:= x \nu \sqrt{2} \rho_{1,2} g(z) \frac{\partial^2}{\partial y \partial z}. \end{aligned}$$

Following [6], we approximate  $u^{\epsilon, \delta}$  by

$$(3.1) \quad \tilde{u}^{\epsilon, \delta} = u_0 + \sqrt{\epsilon} u_{1,0} + \sqrt{\delta} u_{0,1}.$$

First, by matching the powers of  $\epsilon$  and  $\delta$ , we obtain the PDEs satisfied by  $u_0$ ,  $u_{1,0}$  and  $u_{0,1}$ . (We will observe that none of these functions depend on  $y$ ). Next, we will solve these PDEs explicitly. Let  $\langle g(y) \rangle = \int g(y) n(y) dy$ , in which  $n$  is the density of the Gaussian distribution with mean  $m$  and variance  $\nu$ . We denote  $\bar{\sigma}^2(z) = \langle f^2(y, z) \rangle$  and let  $\phi(y, z)$  be the solution of

$$\tilde{\mathcal{L}}_0 \phi(y, z) = f^2(y, z) - \bar{\sigma}^2(z).$$

We find that  $u_0$  solves in (3.1)

$$\begin{cases} \langle \mathcal{L}_2 \rangle u_0 = 0, \\ u_0(T, x; z, s, \xi) = e^{i\xi x}. \end{cases}$$

Note that we see  $z$  as a parameter since  $\mathcal{L}_0$  does not have derivatives with respect to  $z$ . The solution of this PDE can be explicitly obtained as

$$(3.2) \quad u_0(t, x; z, s, \xi) = e^{\alpha(T-t) + \beta(T-t)x},$$

where functions  $\alpha$  and  $\beta$  are defined as

$$\alpha(t) = \frac{\kappa\mu(ac-d)}{bcd} \log \frac{c+de^{bt}}{c+d} + \frac{\kappa\mu}{c}t,$$

$$\beta(t) = \frac{1+ae^{bt}}{c+de^{bt}},$$

in which

$$c = \frac{\kappa + \sqrt{\kappa^2 + 2\bar{\sigma}^2 s}}{-2s},$$

$$d = (1 - ic\xi) \frac{-\kappa + i\bar{\sigma}^2\xi + \sqrt{\kappa^2 + 2\bar{\sigma}^2 s}}{-i2\kappa\xi - \bar{\sigma}^2\xi^2 - 2s},$$

$$a = i(c+d)\xi - 1,$$

$$b = \frac{d(-\kappa - 2cs) + a(-\kappa c + \bar{\sigma}^2)}{ac - d}.$$

The correction term  $u_{1,0}$  in (3.1) solves

$$(3.3) \quad \begin{cases} \langle \mathcal{L}_2 \rangle u_{1,0} = \left\langle \mathcal{L}_1 \tilde{\mathcal{L}}_0^{-1} \frac{1}{x} (\mathcal{L}_2 - \langle \mathcal{L}_2 \rangle) \right\rangle u_0 = \frac{1}{\sqrt{2}} \rho_1 \nu \langle f \phi_y \rangle (z) x \frac{\partial^3 u_0}{\partial x^3}, \\ u_{1,0}(T, x; z, s, \xi) = 0. \end{cases}$$

Observe that  $\frac{\partial^3 u_0}{\partial x^3} = \beta^3(T-t)u_0$ . Letting  $V_1^\epsilon = \sqrt{\epsilon} \frac{1}{\sqrt{2}} \rho_1 \nu \langle f \phi_y \rangle (z)$ , we can write (3.3) as

$$\begin{cases} \langle \mathcal{L}_2 \rangle u_{1,0} = V_1^\epsilon / \sqrt{\epsilon} \beta^3(T-t)u_0, \\ u_{1,0}(T, x; z, s, \xi) = 0. \end{cases}$$

It can be checked that

$$u_{1,0}(t, x; z, s, \xi) = \frac{V_1^\epsilon}{\sqrt{\epsilon}} (D_1(T-t)x + D_2(T-t))u_0(t, x; z, s, \xi).$$

in which  $D_1(t)$  and  $D_2(t)$  are solutions of

$$D_1'(t) + (-\bar{\sigma}^2\beta(t) + \kappa)D_1(t) + \beta^3(t) = 0, \quad D_1(0) = 0,$$

$$D_2'(t) - \kappa\mu D_2(t) = 0, \quad D_2(0) = 0.$$

The correction term  $u_{0,1}$  in (3.1) solves

$$(3.4) \quad \begin{cases} \langle \mathcal{L}_2 \rangle u_{0,1} = -\langle \mathcal{M}_1 \rangle u_0 = -\rho_2 g(z) \langle f \rangle (z) x \frac{\partial^2 u_0}{\partial x \partial z}, \\ u_{0,1}(T, x; z, s, \xi) = 0. \end{cases}$$

We would like to simplify the right hand side if the first equation in (3.4). To this end, observe that  $\frac{\partial u_0}{\partial z}$  solves

$$\begin{cases} \langle \mathcal{L}_2 \rangle \frac{\partial u_0}{\partial z} = -\bar{\sigma}(z)\bar{\sigma}'(z)x \frac{\partial^2 u_0}{\partial x^2} = -\bar{\sigma}(z)\bar{\sigma}'(z)\beta^2(T-t)xu_0, \\ \frac{\partial u_0}{\partial z}(T, x; z, s, \xi) = 0. \end{cases}$$

As a result

$$\frac{\partial u_0}{\partial z} = -\bar{\sigma}(z)\bar{\sigma}'(z)(D_3(T-t)x + D_4(T-t))u_0,$$

where  $D_3(t)$  and  $D_4(t)$  solve

$$\begin{aligned} D_3'(t) + (-\bar{\sigma}^2\beta(t) + \kappa)D_3(t) + \beta^2(t) &= 0, & D_3(0) &= 0, \\ D_4'(t) - \kappa\mu D_3(t) &= 0, & D_4(0) &= 0. \end{aligned}$$

Letting  $V_2^\delta = \sqrt{\delta}\rho_2g(z)\langle f \rangle(z)\bar{\sigma}(z)\bar{\sigma}'(z)$ , we can write (3.4) as

$$\begin{cases} \langle \mathcal{L}_2 \rangle u_{0,1} = V_2^\delta / \sqrt{\delta} ((D_3(T-t) + \beta(T-t)D_4(T-t))xu_0 + D_3(T-t)\beta(T-t)x^2u_0), \\ u_{0,1}(T, x; z, s, \xi) = 0. \end{cases}$$

We seek a solution of form

$$u_{0,1} = \frac{V_2^\delta}{\sqrt{\delta}} (D_5(T-t)x^2 + D_6(T-t)x + D_7(T-t))u_0,$$

and find that  $D_5(t)$ ,  $D_6(t)$ , and  $D_7(t)$  solve the ODEs

$$\begin{aligned} D_5'(t) + 2(-\bar{\sigma}^2\beta(t) + \kappa)D_5(t) + D_3(t)\beta(t) &= 0, & D_5(0) &= 0, \\ D_6'(t) + (-\bar{\sigma}^2\beta(t) + \kappa)D_6(t) - (\bar{\sigma}^2 + 2\kappa\mu)D_5(t) + (D_3(t) + \beta(t)D_4(t)) &= 0, & D_6(0) &= 0, \\ D_7'(t) - \kappa\mu D_6(t) &= 0, & D_7(0) &= 0. \end{aligned}$$

Notice that since the terminal condition is smooth, so the arguments in [6] can be adapted to show that for fixed  $(t, x, y, z)$ , there exists a constant  $C$  such that  $|u^{\epsilon, \delta} - \tilde{u}^{\epsilon, \delta}| < C \cdot (\epsilon + \delta)$ .

Now, let  $\tilde{u}^{(m)} = u_0^{(m)} + \sqrt{\epsilon}u_{1,0}^{(m)} + \sqrt{\delta}u_{0,1}^{(m)}$  be the approximation for  $\mathcal{T}_{t,T}(\theta_1(m + C_t), \xi)$ . We have

$$\begin{aligned} u_0^{(m)} &= e^{\alpha(T-t;m) + \beta(T-t;m)}, \\ \sqrt{\epsilon}u_{1,0}^{(m)} &= V_1^\epsilon (D_1^{(m)}(T-t)x + D_2^{(m)}(T-t))u_0^{(m)}, \\ \sqrt{\delta}u_{0,1}^{(m)} &= V_2^\delta (D_3^{(m)}(T-t)x^2 + D_5^{(m)}(T-t) + D_7^{(m)}(T-t))u_0^{(m)}. \end{aligned}$$

where we have let  $X_t = x$ . We see that the approximation for the loss distribution density and joint distribution density is linear in  $V_1^\epsilon$  and  $V_2^\delta$ :

(3.5)

$$\begin{aligned} \mathbb{P}(N_T - N_t = k | \mathcal{G}_t) &\approx \frac{\Gamma(C_t + k)}{\Gamma(C_t)k!} \sum_{m=0}^k (-1)^{(m)} \binom{k}{m} u_0^{(m)} \\ &+ V_1^\epsilon \frac{\Gamma(C_t + k)}{\Gamma(C_t)k!} \sum_{m=0}^k (-1)^{(m)} \binom{k}{m} (D_1^{(m)}(T-t)x + D_2^{(m)}(T-t)) u_0^{(m)} \\ &+ V_2^\delta \frac{\Gamma(C_t + k)}{\Gamma(C_t)k!} \sum_{m=0}^k (-1)^{(m)} \binom{k}{m} (D_3^{(m)}(T-t)x^2 + D_5^{(m)}(T-t) + D_7^{(m)}(T-t)) u_0^{(m)} \Big|_{\xi=0}, \end{aligned}$$

$$\begin{aligned} \mathbb{P}[N_T - N_t = k, X_T \in dx | \mathcal{G}_t] &\approx \frac{\Gamma(C_t + k)}{\Gamma(C_t)k!} \sum_{m=0}^k \frac{(-1)^m}{2\pi} \binom{k}{m} \int_{-\infty}^{\infty} u_0^{(m)} e^{-ix\xi} d\xi dx \\ &+ V_1^\epsilon \frac{\Gamma(C_t + k)}{\Gamma(C_t)k!} \sum_{m=0}^k \frac{(-1)^m}{2\pi} \binom{k}{m} \int_{-\infty}^{\infty} (D_1^{(m)}(T-t)x + D_2^{(m)}(T-t)) u_0^{(m)} e^{-ix\xi} d\xi dx \\ &+ V_2^\delta \frac{\Gamma(C_t + k)}{\Gamma(C_t)k!} \sum_{m=0}^k \frac{(-1)^m}{2\pi} \binom{k}{m} \int_{-\infty}^{\infty} (D_3^{(m)}(T-t)x^2 + D_5^{(m)}(T-t) + D_7^{(m)}(T-t)) u_0^{(m)} e^{-ix\xi} d\xi dx. \end{aligned}$$

#### 4. STOCHASTIC MEAN REVERSION LEVEL

The dependence of the mean reversion level of  $\lambda$  in (2.2) on  $N$  may reduce the flexibility of the model. This is a side-effect of using the birth process, whose intensity is increasing. Indeed, the disadvantage is clear if we consider the case when the volatility  $\sigma = 0$ . In that case the activity rate process  $X$  follows the dynamics

$$dX_t = \kappa(\mu - X_t)dt.$$

The intensity of  $N_t$  under this assumption follows

$$(4.1) \quad d\lambda_t = \kappa(\mu\eta_t - \lambda_t)dt + \frac{\theta_2}{\eta_t} \lambda_t dN_t,$$

where  $\eta_t = \theta_1 + \theta_2 N_t$ . This setup can be compared to the Hawkes model proposed in [4] and implemented in [9] and [1]. In the Hawkes model, the intensity follows the dynamics

$$d\lambda_t = \kappa(\mu - \lambda_t)dt + \theta dL_t.$$

Recall that  $L_t$  denotes the loss process and is related to  $N_t$  by a constant factor when the loss at default rate is assumed to be constant. While the implementation of the Hawkes process model requires numerical methods, the model specified by (4.1) can be solved analytically. On the other hand, while the Hawkes process model fits to the market data well, see [9], the model described above fits the market data poorly.

We are looking to counteract the effect of the increasing intensity of the birth process by allowing the mean reversion level of the activity rate  $\mu$  to be stochastic. More specifically, we will model the activity rate  $X$  by the solution of

$$dX_t = \kappa(\mu(Y_t, Z_t) - X_t)dt + \sigma\sqrt{X_t}dW_t^0.$$

Here,  $X$  and  $Y$  follow

$$\begin{aligned} dY_t &= \frac{1}{\epsilon} \left( (m - Y_t) - \frac{\nu\sqrt{2}}{\sqrt{\epsilon}} \tilde{\Lambda}(Y_t, Z_t) \right) dt + \frac{\nu\sqrt{2}}{\sqrt{\epsilon}} dW_t^1, \\ dZ_t &= \left( \delta c(Z_t) - \sqrt{\delta} g(Z_t) \tilde{\Gamma}(Y_t, Z_t) \right) dt + \sqrt{\delta} g(Z_t) dW_t^2, \end{aligned}$$

where  $\tilde{\Lambda}$  and  $\tilde{\Gamma}$  are the market prices of the risk of fluctuations in intensity level. As before,  $\epsilon$  and  $\delta$  are small positive constants, and the functions  $c(z)$  and  $g(z)$  are assumed to be smooth. We also assume that  $\mu$  is strictly positive, bounded and smooth. The Brownian motions in the above dynamics are correlated:

$$\mathbb{E}_t[dW_t^0 dW_t^i] = \rho_i dt, \quad i \in \{1, 2\}, \quad \mathbb{E}_t[dW_t^1 dW_t^2] = \rho_{1,2} dt,$$

We need to compute

$$\mathcal{T}_{t,T}(s, \xi) = \mathbb{E}_t \left[ e^{-s \int_t^T X_u du + i\xi X_T} \middle| \mathcal{G}_t \right] = u^{\epsilon, \delta}(t, x, y, z; s, \xi).$$

Thanks to the Feynman-Kac principle, we observe that  $u^{\epsilon, \delta}$  satisfies

$$\begin{cases} \mathcal{L}^{\epsilon, \delta} u^{\epsilon, \delta} = 0, \\ u(T, x, y, z; s, \xi) = e^{i\xi x}, \end{cases}$$

where

$$\mathcal{L}^{\epsilon, \delta} := \frac{1}{\epsilon} \mathcal{L}_0 + \frac{1}{\sqrt{\epsilon}} \mathcal{L}_1 + \mathcal{L}_2 + \sqrt{\delta} \mathcal{M}_1 + \delta \mathcal{M}_2 + \sqrt{\frac{\delta}{\epsilon}} \mathcal{M}_3,$$

in which

$$\begin{aligned} \mathcal{L}_0 &:= \nu^2 \frac{\partial^2}{\partial y^2} + (m - y) \frac{\partial}{\partial y}, \\ \mathcal{L}_1 &:= -\nu\sqrt{2} \tilde{\Lambda}(y, z) \frac{\partial}{\partial y} + \sqrt{2} \nu \rho_1 \sigma \sqrt{x} \frac{\partial^2}{\partial x \partial y}, \\ \mathcal{L}_2 &:= \frac{\partial}{\partial t} + \frac{1}{2} \sigma^2 x \frac{\partial^2}{\partial x^2} + \kappa(\mu(y, z) - x) \frac{\partial}{\partial x} - sx, \\ \mathcal{M}_1 &:= -g(z) \tilde{\Gamma}(y, z) \frac{\partial}{\partial z} + \rho_2 g(z) \sigma \sqrt{x} \frac{\partial^2}{\partial x \partial z}, \\ \mathcal{M}_2 &:= c(z) \frac{\partial}{\partial z} + \frac{1}{2} g^2(z) \frac{\partial^2}{\partial z^2}, \\ \mathcal{M}_3 &:= \nu\sqrt{2} \rho_{1,2} g(z) \frac{\partial^2}{\partial y \partial z}. \end{aligned}$$

We formally expand  $u^{\epsilon, \delta}$  in powers of  $\sqrt{\epsilon}$  and  $\sqrt{\delta}$ :

$$u^{\epsilon, \delta} = u_0 + \sqrt{\epsilon} u_{1,0} + \sqrt{\delta} u_{0,1} + \dots,$$

and further expand  $u_{1,0}$  and  $u_{0,1}$  in powers of  $\sigma$ :

$$u_{1,0} = u_{1,0,0} + \sigma u_{1,0,1} + \dots,$$

$$u_{0,1} = u_{0,1,0} + \sigma u_{0,1,1} + \dots.$$

We approximate  $u^{\epsilon, \delta}$  by

$$(4.2) \quad \tilde{u}^{\epsilon, \delta} = u_0 + \sqrt{\epsilon} u_{1,0,0} + \sqrt{\delta} u_{0,1,0}.$$

We will see that all the correction terms are independent of  $y$ . As in the stochastic volatility case, since the terminal condition is smooth, the arguments in [6] can be adapted to show that for fixed  $(t, x, y, z)$ , there exists a constant  $C$  such that  $|u^{\epsilon, \delta} - \tilde{u}^{\epsilon, \delta}| < C \cdot (\sigma\sqrt{\epsilon} + \sigma\sqrt{\delta} + \epsilon + \delta)$ . We let  $\bar{\mu}(z) = \langle \mu(y, z) \rangle$  and  $\phi(y, z)$  be the solution of

$$\mathcal{L}_0 \phi(y, z) = \mu(y, z) - \bar{\mu}(z).$$

The first correction term  $u_0$  in (4.2) solves

$$\begin{cases} \langle \tilde{\mathcal{L}}_2 \rangle u_0 = 0, \\ u_0(0, x; z, s, \xi) = e^{i\xi x}. \end{cases}$$

where

$$\langle \tilde{\mathcal{L}}_2 \rangle = -\frac{\partial}{\partial \tau} + \frac{1}{2} \sigma^2 x \frac{\partial^2}{\partial x^2} + \kappa(\bar{\mu}(z) - x) \frac{\partial}{\partial x} - sx.$$

and we have let  $\tau = T - t$ . Observe that  $u_0$  can be computed using (3.2). Next, we will compute the correction terms in (4.2). To this end let us denote by  $u_{0,0}$  the solution of

$$\begin{cases} \langle \hat{\mathcal{L}}_2 \rangle u_{0,0} = 0, \\ u_{0,0}(0, x; z, s, \xi) = e^{i\xi x}. \end{cases}$$

where

$$\langle \hat{\mathcal{L}}_2 \rangle = -\frac{\partial}{\partial \tau} + \kappa(\bar{\mu}(z) - x) \frac{\partial}{\partial x} - sx.$$

This first order PDE in  $x$  and  $\tau$  can be determined by method of characteristics, see [10], as

$$u_{0,0}(\tau, x; z, s, \xi) = \exp \left( -s\bar{\mu}(z)\tau + \frac{s}{\kappa}(x - \bar{\mu}(z))(e^{-\kappa\tau} - 1) + i\xi(xe^{-\kappa\tau} + \bar{\mu}(z)(1 - e^{-\kappa\tau})) \right).$$

The correction term  $u_{1,0,0}$  in (4.2) solves

$$(4.3) \quad \begin{cases} \langle \hat{\mathcal{L}}_2 \rangle u_{1,0,0} = \left\langle \hat{\mathcal{L}}_1 \mathcal{L}_0^{-1} (\hat{\mathcal{L}}_2 - \langle \hat{\mathcal{L}}_2 \rangle) \right\rangle u_{0,0} = \frac{V_1^\epsilon}{\sqrt{\epsilon}} \frac{\partial u_{0,0}}{\partial x}, \\ u_{1,0,0}(0, x; z, s, \xi) = 0, \end{cases}$$

in which

$$\hat{\mathcal{L}}_1 := -\nu\sqrt{2}\tilde{\Lambda}(y, z) \frac{\partial}{\partial y},$$

and  $V_1^\epsilon = -\sqrt{\epsilon}\kappa\nu\sqrt{2}\langle \tilde{\Lambda}\phi_y \rangle(z)$ . The right-hand-side of the first equation in (4.3) can be simplified thanks to

$$\frac{\partial u_{0,0}}{\partial x} = \left( \frac{s}{\kappa}(e^{-\kappa\tau} - 1) + i\xi e^{-\kappa\tau} \right) u_{0,0}.$$

On the other hand, the correction term  $u_{0,1,0}$  in (4.2) solves

$$(4.4) \quad \begin{cases} \langle \tilde{\mathcal{L}}_2 \rangle u_{0,1,0} = -\langle \hat{\mathcal{M}}_1 \rangle u_{0,0} = g(z) \langle \tilde{\Gamma} \rangle(z) \frac{\partial u_{0,0}}{\partial z}, \\ u_{0,1,0}(0, x; z, s, \xi) = 0, \end{cases}$$

in which

$$\widehat{\mathcal{M}}_1 := -g(z)\tilde{\Gamma}(y, z)\frac{\partial}{\partial z}.$$

The right-hand side of (4.4) can be simplified by observing that

$$\frac{\partial u_{0,0}}{\partial z} = \bar{\mu}'(z) \left( -s\tau + \left( \frac{s}{\kappa} + i\xi \right) (1 - e^{-\kappa\tau}) \right) u_{0,0}.$$

Letting  $V_2^\delta = \sqrt{\delta}\bar{\mu}'(z)g(z)\langle\tilde{\Gamma}\rangle(z)$ , we can express the initial value problem for  $u_{0,1,0}$  as

$$\begin{cases} \langle\tilde{\mathcal{L}}_2\rangle u_{0,1,0} = \frac{V_2^\delta}{\sqrt{\delta}} \left( -s\tau + \left( \frac{s}{\kappa} + i\xi \right) (1 - e^{-\kappa\tau}) \right) u_{0,0}, \\ u_{0,1,0}(0, x; z, s, \xi) = 0. \end{cases}$$

We recognize that the initial value problems for  $u_{1,0,0}$  and  $u_{0,1,0}$  are again first order PDEs, which can be solved by the method of characteristics. We obtain

$$\begin{aligned} u_{1,0,0} &= \frac{V_1^\epsilon}{\sqrt{\epsilon}} D_1(\tau) u_{0,0}, \\ u_{0,1,0} &= \frac{V_2^\delta}{\sqrt{\delta}} D_2(\tau) u_{0,0}, \end{aligned}$$

where

$$\begin{aligned} D_1(\tau) &= \frac{s}{\kappa^2} (e^{-\kappa\tau} + \tau - 1) + \frac{i\xi}{\kappa} (e^{-\kappa\tau} - 1), \\ D_2(\tau) &= \frac{s\tau^2}{2} + \left( \frac{s}{\kappa} + i\xi \right) \left( \frac{1}{\kappa} (1 - e^{-\kappa\tau}) - \tau \right). \end{aligned}$$

Having obtained the approximation in (4.2) explicitly, we will use it to obtain approximate loss distribution as in (3.5).

## 5. CALIBRATION TO MARKET TRANCHE PRICES

Model calibration involves determining the model parameters

$$\Theta = (X_0, \mu, \kappa, \bar{\sigma}, \theta_1, \theta_2, V_1^\epsilon, V_2^\delta)$$

for the model in Section 3 and

$$\Theta = (X_0, \bar{\mu}, \kappa, \sigma, \theta_1, \theta_2, V_1^\epsilon, V_2^\delta)$$

for the model in Section 4, that yield model prices that best match the market data. We use the CDX.NA.HY.10 (CDX High Yield index portofolio of  $n = 100$  North American constituents) index tranche price data obtained from Bloomberg on June 16, 2008. We take the risk-free rate  $r = 0.03$  (based on the three month LIBOR rate) and the loss at default rate  $l = 0.6$ . The model is fitted to market tranche quotes across maturities of 5yr and 7yr. The goodness-of-fit is measured by the root-mean-squared error (RMSE) defined as:

$$(5.1) \quad \sqrt{\frac{1}{|\Theta|} \sum_k \left( \frac{\text{MarketMid}(k) - \text{Model}(\Theta)}{\text{MarketBid}(k) - \text{MarketAsk}(k)} \right)^2}.$$

where  $|\Theta|$  is the number of data points. We choose the parameters to minimize the RMSE by solving a constrained nonlinear least square problem:

$$\operatorname{argmin}_{\Theta} \sum_k \left( \frac{\text{MarketMid}(k) - \text{Model}(\Theta)}{\text{MarketBid}(k) - \text{MarketAsk}(k)} \right)^2$$

subject to  $2\kappa\mu \geq \bar{\sigma}^2$  for stochastic volatility and  $2\kappa\mu \geq \sigma^2$  for stochastic mean reversion. The denominator in (5.1) is chosen so that the prices with higher liquidity (and therefore a narrower bid-ask spread) have a higher weight. This choice of the denominator is a common practice and is also employed by [9] in Section 7, and [11] on page 22.

Direct implementation of (2.5) and (2.7) using double precision would result in great cancellation errors. Here, we implement high-precision arithmetics in our C++ program. We used the APPREC package, available at <http://crd.lbl.gov/dhbailey/mpdist/>. Implementation of (2.5) also involves discretizing the integral and applying a fast Fourier transform (FFT). For this purpose, we used the fftw package available from <http://www.fftw.org>.

We compare the calibration results for the models in Sections 3 and 4 to the model in Section 2.1, which does not have any stochastic parameter corrections. Our calibration exercise shows that the introduction of the correction terms improves the fit to market data. Our models can also be compared to a bottom-up stochastic volatility intensity model with seven parameters proposed in [7]. This model assumes that the dynamics and the starting points of the intensities are the same for all names in the portfolio. Specifically,

$$\begin{aligned} d\lambda_t^{(i)} &= \kappa(\theta - \lambda_t^{(i)})dt + \sigma(Y_t, Z_t)dW_t^{(i)}, \quad \lambda_t^{(i)} = \lambda; \\ \mathbb{E}[dW_t^{(i)}dW_t^{(j)}] &= \rho dt, \quad i \neq j \end{aligned}$$

The fast process  $Y$  is modeled by

$$dY_t = \frac{1}{\epsilon}(m - Y_t)dt + \frac{\nu\sqrt{2}}{\sqrt{\epsilon}}dW_t^y,$$

and the slow process  $Z$  is modeled by

$$\begin{aligned} dZ_t &= \delta c(Z_t)dt + \sqrt{\delta}g(Z_t)dW_2^z, \\ \mathbb{E}[dW_t^{(i)}dW_t^{(y)}] &= \rho_y dt, \quad \mathbb{E}[dW_t^{(i)}dW_t^{(z)}] = \rho_z dt, \quad \mathbb{E}[dW_t^{(y)}dW_t^{(z)}] = \rho_y dt. \end{aligned}$$

The leading term and correction terms in the approximation for the loss distribution are given explicitly by (13), (32) and (33) in [7], respectively. Our calibration shows that this model overestimates the prices of the equity tranches and underestimate the prices of the senior tranches.

We summarize the data and results of the calibration in Tables 1 and 3. We also plot the loss distribution implied by the Models in Sections 2-4 in Figure 1 and tranche option values implied by these models in Figure 2. We see that the implied loss distribution of our models is bimodal. This captures the observation that the defaults cluster. This type of implied loss distribution was also obtained by [8] (see Figure 2 in that paper), [5] and [2]. We also performed a multi-day analysis, the results of which are reported in Table 2 and Figures 3-5. In the first of the figures we analyze the stability of the fitted parameters of the model in [3]. In Figure 4 we analyze the parameter stability of the stochastic volatility

model proposed in Section 3, and in Figure 5 we show the results of the same analysis for the mean reversion model proposed in Section 4.

## 6. CONCLUSION

In this article, we studied the effect of introducing stochastic parameter fluctuations to time-changed birth process model proposed in [3]. We demonstrated that the extension improves the fit to tranche swap market data across different tranches and maturities (5Y and 7Y) consistently. Calibrations were carried out for different days to demonstrate parameter stability. We observed that our model were able to generate rich shapes the loss distribution, whereas the original model can only give shapes close to binomial distribution. We assumed a separation of time scales of the stochastic fluctuation of parameters, which enables us to reduced the pricing problems to familiar singular-regular perturbation problems. This framework leads to explicit pricing formulas and effective calibration and pricing exotic multi-name, multi-period instruments.

## ACKNOWLEDGMENT

We are grateful to the anonymous referee and the editor Ben Hambly for their careful reading of our paper and their feedback, which helped us improve our paper in significant ways.

## REFERENCES

- [1] Shahriar Azizpour and Kay Giesecke. Self-exciting corporate defaults. Technical report, Stanford University, August 2008. Available at <http://www.stanford.edu/dept/MSandE/people/faculty/giesecke/publications.html>.
- [2] Nordine Bennani. A note on markov functional loss models. Technical report, Dresdner Kleinwort, November 2006. Available at [http://www.defaultrisk.com/pp\\_cdo\\_01.htm](http://www.defaultrisk.com/pp_cdo_01.htm).
- [3] Xiaowei Ding, Kay Giesecke, and Pascal I. Tomecek. Time-changed birth processes and multi-name credit derivatives. *Operations Research*, forthcoming, 2008. Available at <http://www.stanford.edu/dept/MSandE/people/faculty/giesecke/publications.html>.
- [4] Eymen Errais, Kay Giesecke, and Lisa Goldberg. Pricing credit from the top down with affine point process. Technical report, Stanford University, September 2007. Available at <http://www.stanford.edu/dept/MSandE/people/faculty/giesecke/publications.html>.
- [5] Onur Filiz, Xin Guo, Jasaan Morton, and Bernd Sturmfels. Graphical models for correlated defaults. Technical report, University of California, Berkeley, December, 2008. Available at <http://arxiv.org/pdf/0809.1393>.
- [6] Jean-Pierre Fouque, George Papanicolaou, Ronnie Sircar, and Knut Solna. Multiscale stochastic volatility asymptotics. *Multiscale Model. Simul.*, 2(1):22–42 (electronic), 2003.
- [7] Jean-Pierre Fouque, Ronnie Sircar, and Knut Solna. Multiname and multiscale default modeling. Technical report, UCSB, Princeton University, UC Irvine, June 2008. Available at <http://www.princeton.edu/~sircar/Public/ARTICLES>.
- [8] Jean-Pierre Fouque, Brian Wignall, and Xianwen Zhou. Modeling correlated defaults: First passage model under stochastic volatility. *Journal of Computational Finance*, 11(3):43–78, 2008.

- [9] Kay Giesecke and Baeho Kim. Estimating tranche spreads by loss process simulation. *Proceedings of the 2007 Winter Simulation Conference*, pages 967–975, 2007.
- [10] Fritz John. *Partial differential equations*, volume 1 of *Applied Mathematical Sciences*. Springer-Verlag, New York, fourth edition, 1982.
- [11] Evan Papageorgiou and Ronnie Sircar. Multiscale intensity models and name grouping for valuation of multi-name credit derivatives. *Applied Mathematical Finance*, *forthcoming*, March 2008. Available at <http://www.princeton.edu/~sircar>.

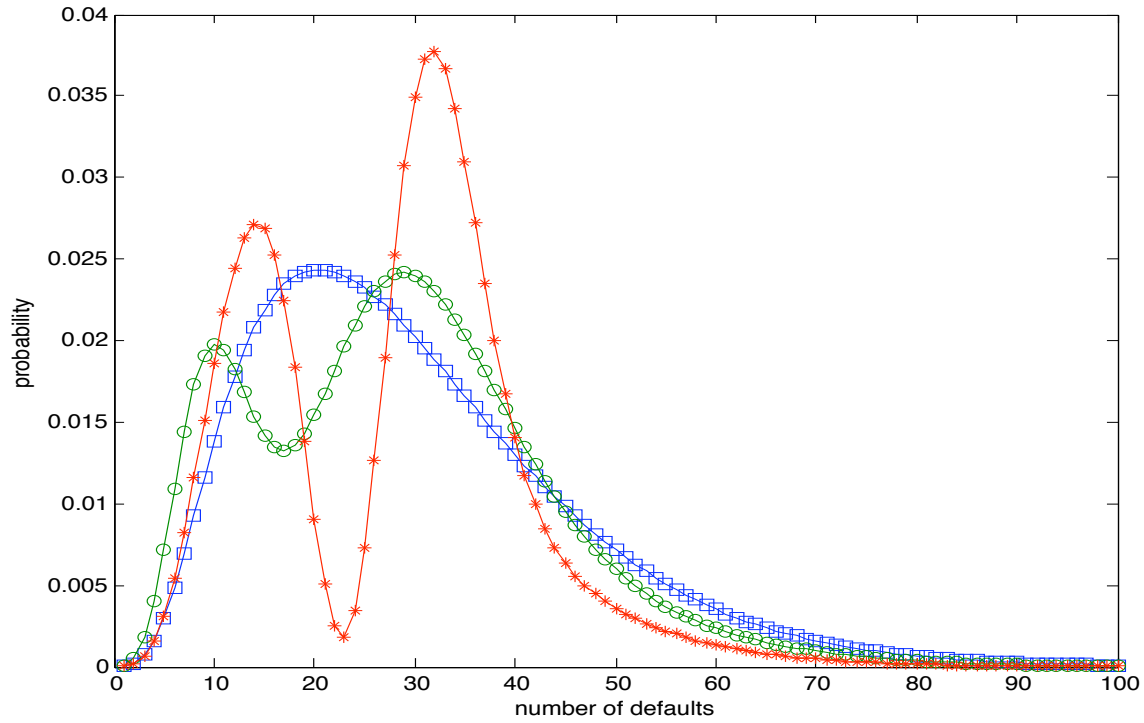


FIGURE 1. 5yr Loss Distribution implied by the models calibrated to 5+7Y CDX.NA.HY.10 June 16, 2008 data.

**Legend**

-squares-, blue(no correction)

'-o', green(stochastic volatility)

'-\*', red(stochastic mean reversion level)

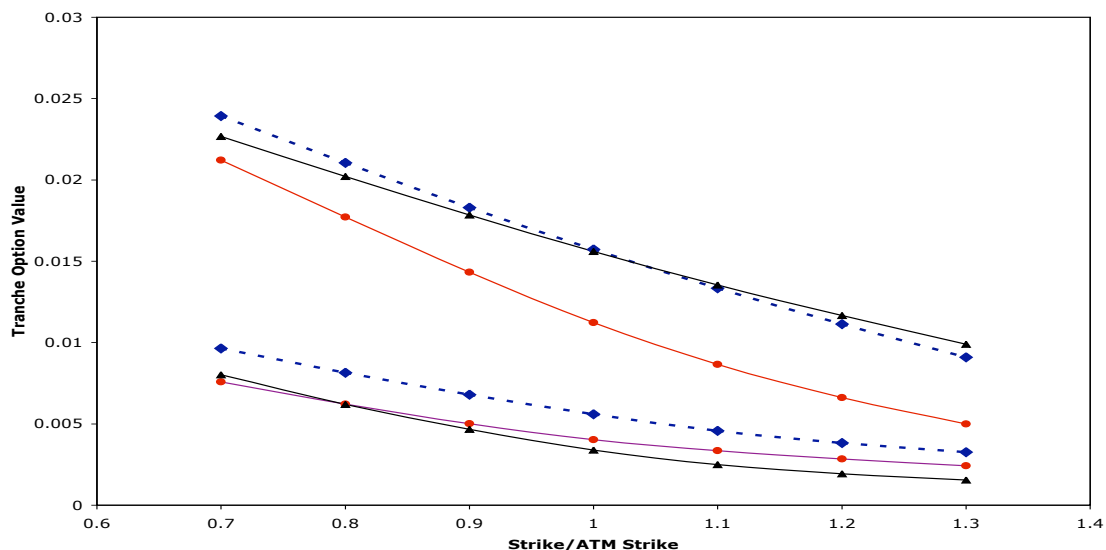


FIGURE 2. Value of option contracts, on the 5 year 15-25 percent and 25-35 percent tranches, implied by the models calibrated to 5+7Y CDX.NA.HY.10 June 16, 2008 data. The options expire in 6 months. These options give the holder the right to enter the CDO swap as a protection buyer. We take ATM=Market Mid=1055bps. Options on 25-35 percent tranche worth less than options on 15-25 percent tranche.

### Legend

- diamonds-, broken blue (no correction)
- filled circles-, red, (stochastic volatility)
- triangles-, black (stochastic mean reversion level)

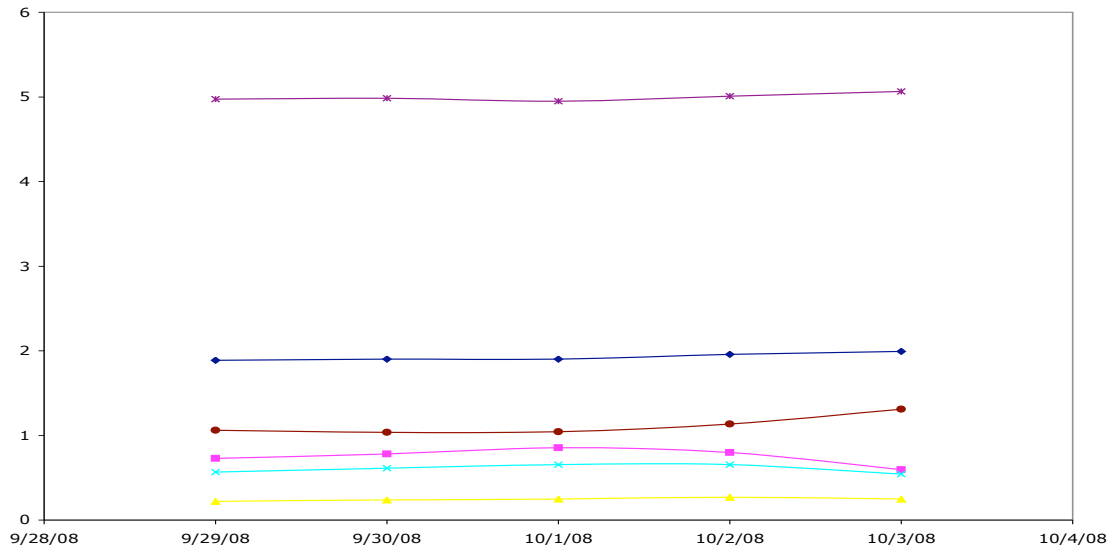


FIGURE 3. Parameter stability: parameters for the model without stochastic fluctuations of the parameters, i.e., the model of [3] are calibrated to 5+7Y CDX.NA.HY.10 September 29, 2008 to October 3, 2008 market data.

**Legend**

- filled diamonds-, dark blue:  $X_0$ .
- filled squares-, pink:  $\mu$ .
- filled triangles-, yellow:  $\kappa$
- x-, light blue:  $\sigma$ .
- star-, purple:  $\theta_1$ .
- filled, circles-, brown:  $\theta_2$ .

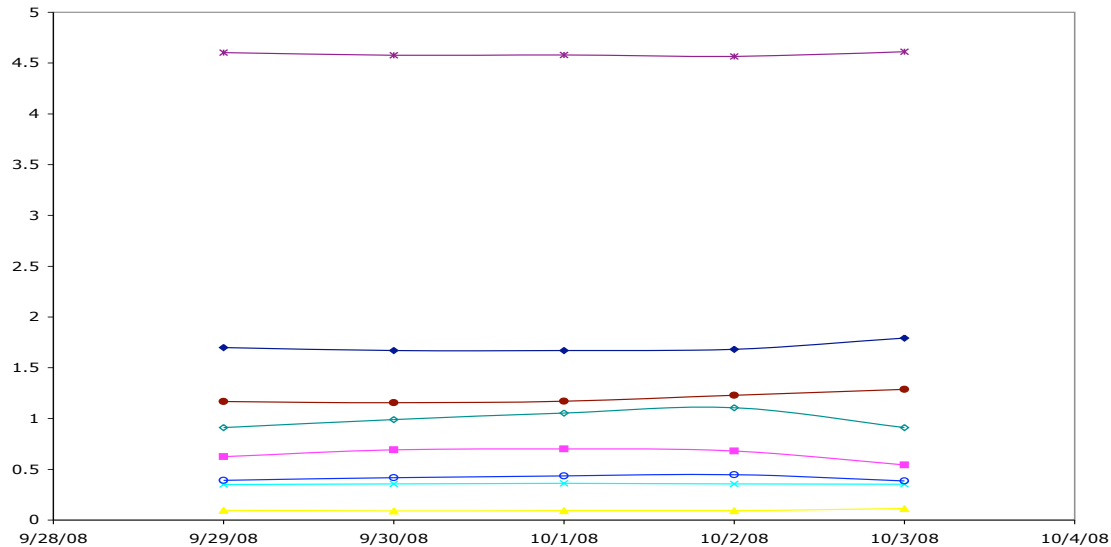


FIGURE 4. Parameter stability: parameters for the model with stochastic volatility, described in Section 3 are calibrated to 5+7Y CDX.NA.HY.10 September 29, 2008 to October 3,2008 market data.

**Legend**

- filled diamonds-, dark blue:  $X_0$ .
- filled squares-, pink:  $\mu$ .
- filled triangles-, yellow:  $\kappa$
- x-,light blue:  $\bar{\sigma}$ .
- star-,purple:  $\theta_1$ .
- filled,circles-,brown:  $\theta_2$ .
- diamonds-:  $V_1^\epsilon$ .
- circles-:  $V_2^\delta$ .

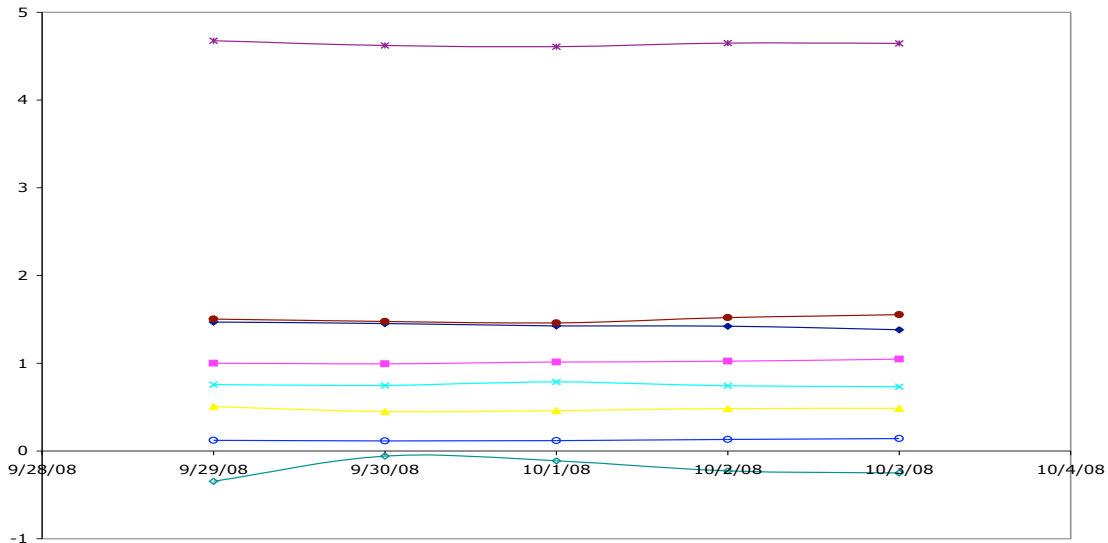


FIGURE 5. Parameter stability: parameters for the model with stochastic mean reversion level, described in Section 4 are calibrated to 5+7Y CDX.NA.HY.10 September 29, 2008 to October 3,2008 market data.

**Legend**

-filled diamonds-, dark blue:  $X_0$ .

-filled squares-, pink:  $\bar{\mu}$ .

-filled triangles-, yellow:  $\kappa$

-x-,light blue:  $\sigma$ .

-star-,purple:  $\theta_1$ .

-filled,circles-,brown:  $\theta_2$ .

-diamonds-:  $V_1^e$ .

-circles-:  $V_2^\delta$ .

Maturity	Contract	MarketBid	MarketAsk	Model1	Model2	Model3	Model4
5Yr	0-10%	88.05%	88.55%	89.92%	87.94%	88.51%	90.65%
	10-15%	66.089%	66.589%	64.24%	66.60%	66.18%	74.62%
	15-25%	1050.29	1059.709	1018.5	1057.3	1061.6	963.4985
	25-35%	523.13	530.38	525.25	528.372	508.4975	85.6576
	35-100%	149.85	154.149	130.0824	148.1399	158.2778	0.0618
7Yr	0-10%	90.849%	91.33%	92.65%	91.47%	92.99%	91.31%
	10-15%	74.73%	75.099%	74.89%	74.97%	74.47%	77.72%
	15-25%	1176.25	1186.25	1118.2	1173.0	1175.7	1271.2
	25-35%	616.69	624.559	690.5859	623.4425	627.8967	301.5964
	35-100%	164.330	168.0	163.9533	167.7249	169.9020	2.0454
RMSE				3.9946	0.5786	1.6869	31.7728

TABLE 1. Calibration results.

The columns “MarketBid” and “MarketAsk” contain the market bid and ask quotes of CDX.NA.HY.10 (CDX High Yield index portfolio of  $n = 100$  North American constituents) on June 16, 2008. Data Source: Bloomberg.

The column of “Model1” contains calibrated prices for the model without stochastic fluctuations of the parameters, i.e, the model of [3].

The column of ”Model2” contains calibrated prices for the model with stochastic volatility, described in Section 3.

The column of “Model3” contains calibrated prices for model with stochastic mean reversion level, described in Section 4.

The column of “Model4” contains calibrated prices for a bottom-up model with stochastic volatility and symmetric names, proposed in [7].

For calibrations, we assumed the risk-free rate  $r = 0.03$  and the loss at default rate  $l = 0.6$ . The calibrated parameters are:

Model1

$$X_0 = 1.4508, \mu = 1.2117, \kappa = 0.1836, \sigma = 0.6670, \theta_1 = 4.6965, \theta_2 = 0.00067895.$$

Model2

$$X_0 = 1.5679, \mu = 0.9502, \kappa = 0.2042, \bar{\sigma} = 0.5054, \theta_1 = 4.6301, \theta_2 = 0.0008758$$

$$V_1^\epsilon = 0.1662, V_2^\delta = 0.0744.$$

Model3

$$X_0 = 1.433, \bar{\mu} = 1.0297, \kappa = 0.8131, \sigma = 1.2650, \theta_1 = 4.6982, \theta_2 = 0.0011$$

$$V_1^\epsilon = -0.2258, V_2^\delta = 0.1102.$$

Model4

$$X_0 = 0.091, \theta = 0.0732, \kappa = 0.4685, \sigma = 0.0469, \rho_X = 0.7825$$

$$V_1(z) = -1.9940e - 07, V_3(z) = -6.5243e - 8.$$

Model	9/29/2008	9/30/2008	10/1/2008	10/2/2008	10/3/2008
Model1	4.2050	4.6205	5.3800	6.4127	4.0369
Model2	1.1367	1.3990	1.8455	2.5738	2.0028
Model3	2.3308	2.2310	2.5772	2.3526	1.8064

TABLE 2. Comparison of goodness of fit measured in RMSE of different models at different dates. Models are calibrated to 5+7Y CDX.NA.HY.10 data from September 29,2008 to October 3,2008. “Model1” refers to the model without stochastic fluctuations of the parameters, i.e., the model of [3]. “Model2” refers to the model with stochastic volatility, described in Section 3. “Model3” contains calibrated prices for model with stochastic mean reversion level, described in Section 4.

Maturity	Contract	MarketBid	MarketAsk	Model1	Model2	Model3	Model4
5Yr	0-10%	92.60%	92.95%	95.66%	93.43%	93.45%	99.38%
	10-15%	77.88%	78.34%	78.16%	77.14%	78.00%	86.99%
	15-25%	1420.6	1428.0	1407.4	1423.6	1427.3	1304.1
	25-35%	726.88	733.75	759.4383	736.157	708.8602	160.3239
	35-100%	214.34	218.16	203.2199	213.3033	230.185	0.2375
7Yr	0-10%	94.54%	94.96%	96.84%	95.27%	96.54%	97.97%
	10-15%	84.06%	84.56%	85.39%	84.46%	83.01%	86.11%
	15-25%	1540.6	1550.6	1510.0	1541.6	1539.9	1600.8
	25-35%	842.6	852.6	892.7707	855.4467	862.7174	440.7766
	35-100%	235.2	240.2	220.622	231.9256	237.2906	4.3973
RMSE				4.2050	1.1367	2.3308	38.7422

TABLE 3. Calibration results.

The columns “MarketBid” and “MarketAsk” contain the market bid and ask quotes of CDX.NA.HY.10 (CDX High Yield index portfolio of  $n = 100$  North American constituents) on September 29, 2008. Data Source: Bloomberg.

The column of “Model1” contains calibrated prices for the model without stochastic fluctuations of the parameters, i.e., the model of [3].

The column of “Model2” contains calibrated prices for the model with stochastic volatility, described in Section 3.

The column of “Model3” contains calibrated prices for the model with stochastic mean reversion level, described in Section 4.

The column of “Model4” contains calibrated prices for a bottom-up model with stochastic volatility and symmetric names, proposed in [7].

For calibrations, we assumed the risk-free rate  $r = 0.0016$  and the loss at default rate  $l = 0.6$ .

The calibrated parameters are:

Model1

$$X_0 = 1.8893, \mu = 0.7273, \kappa = 0.2213, \sigma = 0.5673, \theta_1 = 4.9736, \theta_2 = 0.0011.$$

Model2

$$X_0 = 1.7002, \mu = 0.6238, \kappa = 0.0975, \bar{\sigma} = 0.3488, \theta_1 = 4.6040, \theta_2 = 0.0012$$

$$V_1^\epsilon = 0.0911, V_2^\delta = 0.0392.$$

Model3

$$X_0 = 1.4701, \bar{\mu} = 0.9986, \kappa = 0.5065, \sigma = 0.7579, \theta_1 = 4.677, \theta_2 = 0.0015$$

$$V_1^\epsilon = -0.0345, V_2^\delta = 0.1223.$$

Model4

$$X_0 = 0.0985, \theta = 0.0774, \kappa = 0.4659, \sigma = 0.0492, \rho_X = 0.7851$$

$$V_1(z) = -1.1765792e - 07, V_3(z) = -4.752842e - 8.$$